J|A|C|S
ARTICLES
Published on Web 10/11/2005

Thermoreversible Cis−Cisoidal to Cis−Transoidal Isomerization of Helical Dendronized Polyphenylacetylenes

Virgil Percec,*,† Jonathan G. Rudick,† Mihai Peterca,‡ Martin Wagner,†
Makoto Obata,† Catherine M. Mitchell,† Wook-Dong Cho,†
Venkatachalapathy S. K. Balagurusamy,†,‡ and Paul A. Heiney‡

Contribution from the Roy & Diana Vagelos Laboratories, Department of Chemistry, University of Pennsylvania, Philadelphia, Pennsylvania 19104-6323, and Department of Physics and Astronomy, University of Pennsylvania, Philadelphia, Pennsylvania 19104-6396

Received August 8, 2005; E-mail: percec@sas.upenn.edu

Abstract: High cis content (81−99%) cis−transoidal polyphenylacetylene (PPA) jacketed with amphiphilic self-assembling dendrons, poly[(*3,4−3,5*)*m*G2−4EBn] with $m = 8$, 10, 12, 14, 16, and (*S*)-3,7-dimethyloctyl, were synthesized by Rh(C≡CPh)(nbd)$(PPh_3)_2$ (nbd = 2,5-norbornadiene)/*N,N*-(dimethylamino)pyridine (DMAP) catalyzed polymerization of macromonomers. The resulting cylindrical PPAs self-organize into hexagonal columnar lattices with intracolumnar order (Φ_h^{io}) and without (Φ_h). The polymers with $m = 12$, 14, and 16 exhibit also a hexagonal columnar crystal phase ($\Phi_{h,k}$). The reversible $\Phi_{h,k}$-to-Φ_h^{io}-to- Φ_h phase transition in these dendronized PPAs was analyzed by a combination of differential scanning calorimetry and small and wide-angle X-ray diffraction experiments performed on powder and oriented fibers. In the $\Phi_{h,k}$ and Φ_h^{io} phases, the dendronized PPAs form helical porous columns. The helical pore disappears in the Φ_h phase. This change is accompanied by a decrease of the external column diameter that is induced by stretching of the polymer backbone along the axis of the cylinder. The helix sense of the porous PPA is selected by homochiral alkyl dendritic tails. This transition is generated by an unprecedented conversion of the PPA backbone from the cis−cisoidal conformation in the $\Phi_{h,k}$ and Φ_h^{io} phases to the cis−transoidal conformation in the Φ_h phase. Under the same conditions, the pristine cis-PPA undergoes cis−trans isomerization and irreversible intramolecular 6π electrocyclization of 1,3-*cis*,5-hexatriene sequences followed by chain cleavage. These processes are eliminated in the dendronized cis-PPA below its decomposition temperature.

Introduction

Dendronized polymers approach the architectural complexity of biomacromolecules and the dimensions required for molecular nanoscale construction.[1] Composed of a linear polymer backbone jacketed by dendritic appendages on every repeat unit, dendronized polymers are prepared via divergent,[2] attach-to,[3] or macromonomer strategies.[3b,4,5,6] More recently, noncovalent interactions have been employed in an attach-to strategy[7] and to self-assemble dendronized supramolecular polymers.[8] Polymerization of convergently synthesized dendritic macromonomers renders the highest degree of structural perfection, particularly when combined with living polymerizations.[4] Regardless of the synthetic method employed, two classes of dendrons have been used in the construction of dendronized polymers: self-assembling[4a−f,5c,j,l−o,6,7a,8] and non-self-assembling.[2,3b,c,4g,h,5a,b,d−i,k] In solution, dendronized polymers adopt a cylindrical structure whose stiffness and microenvironment are determined by the dendritic side chain.[2a,c,3b,5k,6c] Less well-defined structures are obtained in bulk.[1,5b,c,h,k] We have elaborated a strategy to overcome this limitation by jacketing polymers with self-assembling dendrons that produce periodic order in the bulk state.[3a,4a−f,6,7a] The resulting polymers display a diversity of shapes that self-organize into one-dimensional (1-D) smectic, two-dimensional (2-D) *p*6*mm* hexagonal, *p*2*mm* simple rectangular, and *c*2*mm* centered rectangular columnar,

† Department of Chemistry, University of Pennsylvania.
‡ Department of Physics and Astronomy, University of Pennsylvania.

(1) For selected reviews on dendronized polymers, see: (a) Schlüter, A. D. *Topics Curr. Chem.* **2005**, *245*, 151−191. (b) Frauenrath, H. *Prog. Polym. Sci.* **2005**, *30*, 325−384. (c) Ishizu, K.; Tsubaki, K.; Mori, A.; Uchida, S. *Prog. Polym. Sci.* **2002**, *28*, 27−54. (d) Grayson, S. M.; Fréchet, J. M. J. *Chem. Rev.* **2001**, *101*, 3819−3867. (e) *Dendrimers and Other Dendritic Polymers*. Fréchet, J. M. J., Tomalia, D. A., Eds. Wiley: Chichester, New York, 2001. (f) Sheiko, S. S.; Möller, M. *Chem. Rev.* **2001**, *101*, 4099−4123. (g) Schlüter, A. D.; Rabe, J. P. *Angew. Chem., Int. Ed.* **2000**, *39*, 864−883. (h) Percec, V.; Ahn, C.-H.; Cho, W.-D.; Johansson, G.; Schlueter, D. *Macromol. Symp.* **1997**, *118*, 33−43. (i) Percec, V.; Heck, J.; Johansson, G.; Tomazos, D.; Kawasumi, M.; Ungar, G. *J. Macromol. Sci., Pure Appl. Chem.* **1994**, *A31*, 1031−1070.

(2) For examples of the divergent synthetic strategies, see: (a) Tomalia, D. A.; Kirchhoff, P. M. U.S. Patent 4,694,064, 1987; (b) Yin, R.; Zhu, Y.; Tomalia, D. A.; Ibuki, H. *J. Am. Chem. Soc.* **1998**, *120*, 2678−2679. (c) Ouali, N.; Méry, S.; Skoulios, A.; Noirez, L. *Macromolecules* **2000**, *33*, 6185−6193. (d) Grayson, S. M.; Fréchet, J. M. J. *Macromolecules* **2001**, *34*, 6542−6544. (e) Malkoch, M.; Carlmark, A.; Woldegiorgis, A.; Hult, A.; Malmström, E. E. *Macromolecules* **2004**, *37*, 322−329.

(3) For examples of the attach-to synthetic strategies, see: (a) Percec, V.; Heck, J.; Ungar, G. *Macromolecules* **1991**, *24*, 4957−4962. (b) Karakaya, B.; Claussen, W.; Gessler, K.; Saenger, W.; Schlüter, A.-D. *J. Am. Chem. Soc.* **1997**, *119*, 3296−3301. (c) Zhuravel, M. A.; Davis, N. E.; Nguyen, S. T.; Koltover, I. *J. Am. Chem. Soc.* **2004**, *126*, 9882−9883.

Scheme 1

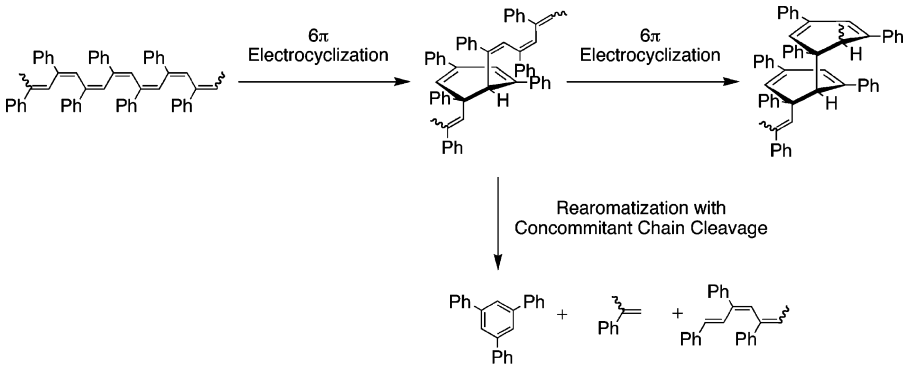

and three-dimensional (3-D) $Pm\bar{3}n$ cubic, $\{Im\}\bar{3}n$ cubic, $P4_{2/mnm}$ tetragonal, and 12-fold symmetry lattices.[4a−f,6,7,9]

Efforts are under way to understand the evolution of homochirality at interfaces.[8,10,11] Polymers adopting a preferred helical screw sense are of particular interest because individual molecules might be resolved by scanning tunneling (STM) and atomic force (AFM) microscopy.[11] Cis−transoidal polyphenylacetylenes (PPAs) adopt a helical conformation[12a,13] whose screw sense is selected by incorporation of chiral substituents or by complexation of chiral substrates.[14] Visualization of predominantly single-handed helical superstructures on mica or highly ordered pyrolytic graphite (HOPG) corroborates solution spectroscopy but is limited by irreversible structural changes undergone by the polymer during visualization.[11d,e] Intramolecular cyclization via 6π electrocyclization of 1,3-*cis*,5-hexatriene sequences in the PPA backbone generate cyclohexadiene repeat units at temperatures as low as 20 °C in solution (Scheme 1).[12] Re-aromatization of the cyclohexadiene moiety results in extrusion of triarylbenzene and concomitant chain cleavage at higher temperatures.[12] A second chain cleavage event occurs in solutions exposed to O_2 and ambient light, which likely proceeds via direct oxidation of the polyene backbone[12d] (not shown in Scheme 1).

Direct visualization of dendron-jacketed polymers offers the opportunity to quantitatively probe fundamental questions about molecular conformation and the formation of 1-D, 2-D, and 3-D periodic states.[1f] Retrostructural analysis of the bulk self-organized lattices confirms that single molecules are investigated and permits rational design of polymers with controlled shape, stiffness, and size that can reverse traditional trends encountered in their pristine macromolecules.[6b] Previous studies of flexible polymer backbones jacketed with self-assembling dendrons have elucidated the mechanism for shape evolution.[4c,6a−c] Macromonomers derived from flat-tapered dendrons form disc-shaped oligomers (i.e., $L \ll a$, where L is the length of the chain and a is the lattice parameter, which is the same as the diameter of a cylindrical macromolecule). Longer oligomers ($L < a$) behave as short, flexible stacks. Polymers of a given degree of polymerization (DP) exhibit rodlike character when $L > a$ and become stiff when $L \gg a$. Polymerization of macromonomers containing conical dendrons generate fragments of sphere when DP $< \mu'$ (where μ' is the number of dendrons in a single spherical object). In the ideal case where DP $= \mu'$, the spherical object is a single macromolecule. When DP $> \mu'$, quasi-equivalence of flat-tapered and conical dendrons allows the object to adopt a cylindrical shape whose stiffness is attenuated by the size of the dendritic side chain. On the basis of conformational analysis of visualized dendronized polymers and geometrical arguments, the polymer backbone penetrating a cylindrical object can adopt a helical conformation.[1f,6]

(4) For examples of dendritic macromonomers polymerized using various living methods, see: (a) Percec, V.; Heck, J.; Lee, M.; Ungar, G.; Alvarez-Castillo, A. *J. Mater. Chem.* **1992**, *2*, 1033−1039. (b) Percec, V.; Obata, M.; Rudick, J. G.; De, B. B.; Glodde, M.; Bera, T. K.; Magonov, S. N.; Balagurusamy, V. S. K.; Heiney, P. A. *J. Polym. Sci., Part A: Polym. Chem.* **2002**, *40*, 3509−3533. (c) Percec, V.; Schlueter, D. *Macromolecules* **1997**, *30*, 5783−5790. (d) Percec, V.; Holerca, M. N.; Magonov, S. N.; Yeardley, D. J. P.; Ungar, G.; Duan, H.; Hudson, S. D. *Biomacromolecules* **2001**, *2*, 706−728. (e) Percec, V.; Holerca, M. N. *Biomacromolecules* **2000**, *1*, 6−16. (f) Duan, H.; Hudson, S. D.; Ungar, G.; Holerca, M. N.; Percec, V. *Chem.-Eur. J.* **2001**, *7*, 4134−4141. (g) Zhang, A.; Zhang, B.; Wächtersbach, E.; Schmidt, M.; Schlüter, A. D. *Chem.-Eur. J.* **2003**, *9*, 6083−6092. (h) Zhang, A.; Wei, L.; Schlüter, A. D. *Macromol. Rapid Commun.* **2004**, *25*, 799−803.

(5) For examples of the dendritic macromonomer strategies, see: (a) Draheim, G.; Ritter, H. *Macromol. Chem. Phys.* **1995**, *196*, 212−222. (b) Jahromi, S.; Coussens, B.; Meijerink, N.; Braam, A. W. M. *J. Am. Chem. Soc.* **1998**, *120*, 9753−9762. (c) Bao, Z.; Amundson, K. R.; Lovinger, A. J. *Macromolecules* **1998**, *31*, 8647−8649. (d) Sato, T.; Jiang, D.-L.; Aida, T. *J. Am. Chem. Soc.* **1999**, *121*, 10658-10659. (e) Setayesh, S.; Grimsdale, A. C.; Weil, T.; Enkelmann, V.; Müllen, K.; Meghdadi, F.; List, E. J. W.; Leising, G. *J. Am. Chem. Soc.* **2001**, *123*, 946−953. (f) Marsitzky, D.; Vestberg, R.; Blainey, P.; Tang, B. T.; Hawker, C. J.; Carter, K. R. *J. Am. Chem. Soc.* **2001**, *123*, 6965−6972. (g) Kim, H.-J.; Zin, W.-C.; Lee, M. *J. Am. Chem. Soc.* **2004**, *126*, 7009−7014. (h) Kaneko, T.; Horie, T.; Asano, M.; Aoki, T.; Oikawa, E. *Macromolecules* **1997**, *30*, 3118−3121. (i) Kaneko, T.; Asano, M.; Yamamoto, K.; Aoki, T. *Polym. J.* **2001**, *33*, 879−890. (j) Schenning, A. P. H. J.; Fransen, M.; Meijer, E. W. *Macromol. Rapid Commun.* **2002**, *23*, 265−270. (k) Förster, S.; Neubert, I.; Schlüter, A. D.; Lindner, P. *Macromolecules* **1999**, *32*, 4043−4049. (l) Percec, V.; Schlueter, D.; Ungar, G.; Cheng, S. Z. D.; Zhang, A. *Macromolecules* **1998**, *31*, 1745−1762. (m) Percec, V.; Heck, J.; Ungar, G. *Macromolecules* **1991**, *24*, 4957. (n) Percec, V.; Heck, J.; Tomazos, D.; Falkenberg, F.; Blackwell, H.; Ungar, G. *J. Chem. Soc., Perkin Trans. 1* **1993**, 2799. (o) Percec, V.; Tomazos, D.; Heck, J.; Blackwell, H.; Ungar, G. *J. Chem. Soc., Perkin Trans. 2* **1994**, 31.

(6) For examples of polystyrene dendronized with self-assembling monodendrons, see: (a) Percec, V.; Ahn, C.-H.; Barboiu, B. *J. Am. Chem. Soc.* **1997**, *119*, 12978-12979. (b) Percec, V.; Ahn, C.-H.; Ungar, G.; Yeardley, D. J. P.; Möller, M.; Sheiko, S. S. *Nature* **1998**, *391*, 161−164. (c) Percec, V. et al. *J. Am. Chem. Soc.* **1998**, *120*, 8619−8631. (d) Prokhorova, S. A.; Sheiko, S. S.; Möller, M.; Ahn, C.-H.; Percec, V. *Macromol. Rapid Commun.* **1998**, *19*, 359−366. (e) Prokhorova, S. A.; Sheiko, S. S.; Mourran, A.; Azumi, R.; Beginn, U.; Zipp, G.; Anh, C.-H.; Holerca, M. N.; Percec, V.; Möller, M. *Langmuir* **2000**, *16*, 6862−6867. (f) Rapp, A.; Schnell, I.; Sebastiani, D.; Brown, S. P.; Percec, V.; Spiess, H. W. *J. Am. Chem. Soc.* **2003**, *125*, 13284−13297. (g) Prokhorova, S. A.; Sheiko, S. S.; Ahn, C.-H.; Percec, V.; Möller, M. *Macromolecules* **1999**, *32*, 2653−2660.

(7) For examples of noncovalent attach-to strategies, see: (a) Percec, V.; Glodde, M.; Bera, T. K.; Miura, Y.; Shiyanovskaya, I.; Singer, K. D.; Spiess, H.-W.; Hudson, S. D.; Duan, H. *Nature* **2002**, *419*, 384−387. (b) Bilibin, A. Y.; Moukhina, I. V.; Girbasova, N. V.; Egorova, G. G. *Macromol. Chem. Phys.* **2004**, *205*, 1660−1666. (c) Kamikawa, Y.; Kato, T.; Onouchi, H.; Kashiwagi, D.; Maeda, K.; Yashima, E. *J. Polym. Sci., Part A: Polym. Chem.* **2004**, *42*, 4580−4586.

(8) Percec, V.; et al. *Nature* **2004**, *430*, 764−768.

(9) (a) Zeng, X.; Ungar, G.; Liu, Y.; Percec, V.; Dulcey, A. E.; Hobbs, J. K. *Nature* **2004**, *428*, 157−160. (b) Ungar, G.; Liu, Y.; Zeng, X.; Percec, V.; Cho, W.-D. *Science* **2003**, *299*, 1208−1211.

(10) Mamdouh, W.; Uji-i, H.; Dulcey, A. E.; Percec, V.; De Feyter, S.; De Schryver, F. C. *Langmuir* **2004**, *20*, 7678−7685.

Scheme 2 [a]

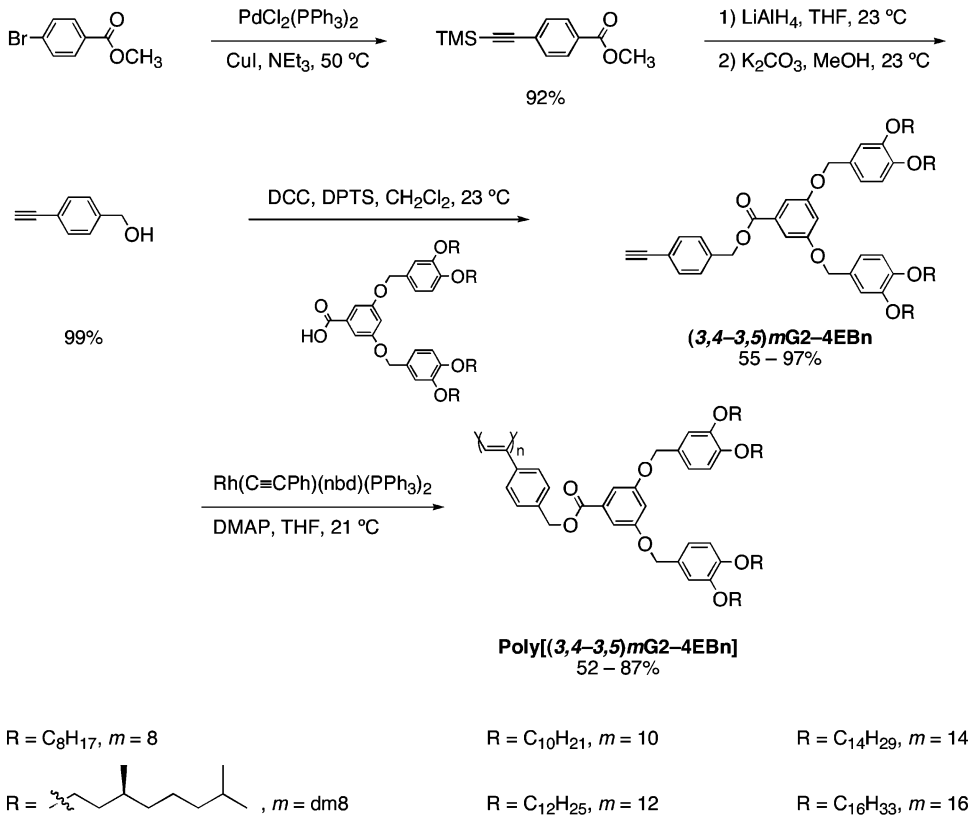

[a] DPTS = *N*,*N*-dimethylaminopyridinium tosylate; nbd = 2,5-norbornadiene; DMAP = *N*,*N*-(dimethylamino)pyridine.

We have prepared a library of dendronized cis−transoidal PPAs to examine helix selection within the cylindrical object. Herein, we report cis−transoidal PPAs jacketed with a particular dendron substitution pattern that matches the helical pitch of the pristine PPA. Experimental observations in the solid state and solution demonstrate helical porous order within the cylindrical object. At elevated temperatures, the polymer undergoes an unprecedented cis−cisoidal-to-cis−transoidal conformational isomerization that closes the pore and circumvents the intramolecular 6π electrocyclization occurring in pristine cis-PPA. This isomerization is reversible. Structural analysis confirms that molecular weight and cis content of dendronized PPAs remain unchanged, thus providing a gating mechanism for the porous structure.

Results and Discussion

Synthesis. The self-assembling macromonomers, **(***3,4-3,5***)-***m*G2−4EBn with m = 8, 10, 12, 14, 16, and (*S*)-3,7-dimethyloctyl were selected from a library designed by analogy to our previously reported dendronized polystyrenes.[6] Synthesis and polymerization of the dendritic macromonomers are illustrated in Scheme 2. The polymerizable apex was synthesized according to modified literature procedures.[15] Methyl 4-bromobenzoate was subjected to Pd-catalyzed Sonogashira cross-coupling with trimethylsilylacetylene. Purification of the disubstituted acetylene by sublimation was employed to avoid side reactions related to trace metal impurities. Sequential reduction of the methyl ester with $LiAlH_4$ followed by desilylation in basic methanol provided the desired 4-ethynylbenzyl alcohol (**4EBnOH**), which was also purified by sublimation. The synthesis and structural analysis of **(***3,4-3,5***)**12G2−CO_2H was reported previously.[6c] Preparation of dendrons with the same substitution pattern and different alkyl tails was accomplished using the same

Table 1. Structural Analysis of **Poly[(*3,4-3,5*)*m*G2−4EBn]**

m	DP_{th} [a]	M_n [b]	M_w/M_n [b]	cis content [c]
8	48	45 400	1.28	99%
dm8	53	49 000	1.38	95%
10	56	101 000	1.35	81%
12	52	61 300	1.22	87%
14	49	50 000	1.24	91%
16	52	—[d]	—[d]	99%

[a] Theoretical degree of polymerization = $[\mathbf{4EBn}]_0/[Rh]_0$. [b] Determined by GPC (THF, 1 mL/min) calibrated with polystyrene standards. [c] Determined as prescribed in ref 12a. [d] Insoluble in THF.

(11) (a) Li, B. S.; Cheuk, K. K. L.; Ling, L.; Chen, J.; Xiao, X.; Bai, C.; Tang, B. Z. *Macromolecules* **2003**, *36*, 77−85. (b) Sakurai, S.-i.; Kuroyanagi, K.; Morino, K.; Kunitake, M.; Yashima, E. *Macromolecules* **2003**, *36*, 9670−9674. (c) Shinohara, K.-I.; Yasuda, S.; Kato, G.; Fujita, M.; Shigekawa, H. *J. Am. Chem. Soc.* **2001**, *123*, 3619−3620. (d) Shinohara, K.-i.; Kitami, T.; Nakamae, K. *J. Polym. Sci., Part A: Polym. Chem.* **2004**, *42*, 3930−3935.

(12) (a) Simionescu, C. I.; Percec, V.; Dumitrescu, S. *J. Polym. Sci., Polym. Chem. Ed.* **1977**, *15*, 2497−2509. (b) Percec, V. *Polym. Bull.* **1983**, *10*, 1−7. (c) Percec, V.; Rudick, J. G.; Nombel, P.; Buchowicz, W. *J. Polym. Sci., Part A: Polym. Chem.* **2002**, *40*, 3212−3220. (d) Percec, V.; Rudick, J. G. *Macromolecules* **2005**, *38*, 7241−7250. (e) Simionescu, C. I.; Percec, V. *J. Polym. Sci. Polym. Chem. Ed.* **1980**, *18*, 147−155. (f) Percec, V.; Rudick, J. G.; Aqad, E. *Macromolecules* **2005**, *38*, 7205−7206.

(13) (a) Nakano, T.; Okamoto, Y. *Chem. Rev.* **2001**, *101*, 4013−4038. (b) Cornelissen, J. J. L.; Rowan, A. E.; Nolte, R. J. M.; Sommerdijk, N. A. J. M. *Chem. Rev.* **2001**, *101*, 4039−4070. (c) Yashima, E.; Maeda, K.; Nishimura, T. *Chem.-Eur. J.* **2004**, *10*, 42−51.

(14) (a) Aoki, T.; Kokai, M.; Shinohara, K.-i.; Oikawa, E. *Chem. Lett.* **1993**, 2009−2012. (b) Yashima, E.; Maeda, K.; Okamoto, Y. *Nature* **1999**, *399*, 449−451.

(15) (a) Landgrebe, J. A.; Rynbrandt, R. H. *J. Org. Chem.* **1966**, *31*, 2585−2593. (b) Austin, W. B.; Bilow, N.; Kelleghan, W. J.; Lau, K. S. Y. *J. Org. Chem.* **1981**, *46*, 2280−2286.

Table 2. Thermal Analysis of **Poly[(*3,4-3,5*)*m*G2−4EBn]** by Differential Scanning Calorimetry

polymer	thermal transitions (°C) and corresponding enthalpy changes (kcal/mol)[a]
poly[(*3,4-3,5*)8G2−4EBn]	$\Phi_{h,g}^{io}$,[b] 46 (0.56); Φ_h^{io},[c] 96 (1.26); Φ_h,[d] 130 dec[e]
poly[(*3,4-3,5*)dm8G2−4EBn]	$\Phi_{h,g}$,[f] 50; Φ_h, 120 dec
poly[(*3,4-3,5*)10G2−4EBn]	$\Phi_{h,g}$,[f] 37 (0.38); Φ_h, 60 (−0.35); Φ_h^{io}, 91 (1.25); Φ_h, 130 dec
poly[(*3,4-3,5*)12G2−4EBn]	$\Phi_{h,k}$,[g] 0 (3.63); Φ_h^{io}, 88 (1.11); Φ_h, 140 dec
poly[(*3,4-3,5*)14G2−4EBn]	$\Phi_{h,k}$, 24 (5.63); Φ_h^{io}, 87 (0.50); Φ_h, 120 dec
poly[(*3,4-3,5*)16G2−4EBn]	$\Phi_{h,k}$, 49 (12.71); Φ_h^{io}, 89 (1.66); Φ_h, 140 dec

[a] Data from second heating DSC scans at 10 °C/min. [b] $\Phi_{h,g}^{io}$, glassy state of hexagonal columnar lattice with intracolumnar order. [c] Φ_h^{io}, hexagonal columnar lattice with intracolumnar order. [d] Φ_h, hexagonal columnar lattice. [e] dec, onset of decomposition. [f] $\Phi_{h,g}$, glassy state of hexagonal columnar lattice. [g] $\Phi_{h,k}$ columnar hexagonal crystal.

convergent synthetic strategy. The macromonomers were prepared by condensation of each of the dendritic carboxylic acids with **4EBnOH** following the method of Moore and Stupp.[16]

Synthesis and structural analysis of the four possible PPA isomers (i.e., cis−cisoidal, cis−transoidal, trans−cisoidal and trans−transoidal) was demonstrated using Ziegler−Natta-type catalysts.[12] Catalysts based on Rh(I) have emerged as a convenient method for stereoselective preparation of cis−transoidal PPA.[17] We are particularly interested in living polymerization methods for preparation of dendronized polymers.[4a−f] Only a few Rh-based catalysts have been reported to exhibit characteristics of a living polymerization of arylacetylene monomers.[17a] Noyori and co-workers have shown that Rh(C≡CPh)(nbd)$(PPh_3)_2$ (nbd = 2,5-norbornadiene), in the presence of 10 equiv of *N*,*N*-(dimethylamino)pyridine (DMAP), induces stereospecific polymerization of arylacetylenes with controlled molecular weight, narrow molecular weight distribution (M_w/M_n), and chain ends active for reinitiation.[18] We have employed this catalytic system to prepare the dendronized PPAs (Scheme 2).

Two methods for the analysis the cis and trans contents of PPA have been advanced.[12a,b] The more detailed method[12b] accounts for the fractions of cis-polyene, trans-polyene, and cyclohexadiene repeat units formed during polymerization and purification. The resonance for the methine proton of cyclohexadiene repeat units is broad and found in the range 4.5−3 ppm. Due to overlap with the alkyl ether proton resonances associated with the alkyl tails (3.8 ppm in $CDCl_3$), the broad, weak resonance due to cyclohexadiene repeat units cannot be integrated reliably. A simplified analysis determines cis content[12a] by the ratio of the integrated area for the resonance at 5.8 ppm to all resonances in the range 7.2−5.5 ppm (i.e., all aromatic and vinylic resonances). This approach overlooks the overlap of cis-polyene resonances with vinylic resonances from cyclohexadiene repeat units but offers a reasonable index for the structural composition of PPAs. Table 1 summarizes the molecular weight and structural composition of the polymer.

Relative molecular weight (M_n) and molecular weight distribution (M_w/M_n) determined by gel permeation chromatography (GPC) relative to polystyrene standards are reported in Table 1. Absolute molecular weight determination by light scattering on polystyrenes and polymethacrylates jacketed with self-assembling dendrons confirmed that GPC results obtained with polystyrene standards underestimate the true molecular weight.[6] We and others have noted this behavior with a range of dendron−polymer backbone combinations.[2c,d,4b,d,g,5k] Additionally, we have shown that extremely high molecular weight fractions exhibit anomalous elution behavior.[6c] With regard to the present polymers, we do not anticipate such behavior. Considering the theoretical DP based on the ratio of monomer to Rh and the previously noted low initiator efficiency, the dendronized PPAs considered here are significantly shorter than the corresponding dendronized polystyrene.

Structural and Retrostructural Analysis. Differential scanning calorimetry (DSC) and thermal optical polarized microscopy (TOPM) were used to confirm the presence of hexagonal columnar phases. Table 2 summarizes the phase behavior determined by DSC. Increasing number of methylene units (*m*) in the alkyl tails raises the melting temperature, such that crystalline phases are observed for $m = 12$, 14, and 16. In all cases, decomposition occurs before isotropization. Nonetheless, reversible heating and cooling cycles can be obtained if the maximum temperature is kept 20 °C below the observed decomposition temperature. While all of the dendronized PPAs exhibit minor inflections during the first heating cycle that are due to various thermal history events, only the hexagonal columnar crystal ($\Phi_{h,k}$) to Φ_h^{io} ($m = 12$, 14, and 16) and Φ_h^{io}−Φ_h phase transitions are reversible and reproducible during all subsequent scans. In addition, exothermic transitions on heating ($m = 10$) due to kinetic effects induced by close proximity to glass transition and chain stiffness are sometimes observed.[17b]

Hexagonal columnar phases identified by the combination of DSC and thermal optical polarized microscopy (TOPM) were assigned by X-ray diffraction (XRD). Table 3 enumerates the lattice symmetry, observed *d*-spacings, lattice parameter (*a*), experimental density at 20 °C (ρ_{20}), and number of dendrons per column stratum. For all peripheral alkyl chain variations, a hexagonal columnar (Φ_h) phase is observed. While several thermal transitions are observed during the first heating cycle, the lattice parameter changes very little except through the highest temperature transition. The corresponding change in lattice parameter cannot be explained exclusively by the contraction of the peripheral alkyl chains.

An intracolumnar microphase-segregated model consisting of a disordered liquidlike aliphatic coat jacketing the aromatic part of the dendron has been demonstrated for both macromolecular[4d,5l] and supramolecular[19] columns generated from self-assembling dendritic building blocks. In the Φ_h phase, the aromatic part of the dendron is also disordered liquidlike. However, in the Φ_h^{io} phase, the aromatic part displays intra-

(16) Moore, J. S.; Stupp, S. I. *Macromolecules* **1990**, *23*, 65−70.
(17) (a) Sedlácek, J.; Vohlídal, J. *Collect. Czech. Chem. Commun.* **2003**, *63*, 1745−1790. (b) Percec, V.; Keller, A. *Macromolecules* **1990**, *23*, 4347−4350.
(18) (a) Kishimoto, Y.; Eckerle, P.; Miyatake, T.; Ikariya, T.; Noyori, R. *J. Am. Chem. Soc.* **1994**, *116*, 12131-12132. (b) Kishimoto, Y.; Eckerle, P.; Miyatake, T.; Kainosho, M.; Ono, A.; Ikariya, T.; Noyori, R. *J. Am. Chem. Soc.* **1999**, *121*, 12035−12044.
(19) Ungar, G.; Abramic, D.; Percec, V.; Heck, J. A. *Liq. Cryst.* **1996**, *21*, 73−86.

Table 3. Measured *d* Spacings and Structural Analysis of the Hexagonal Columnar Lattices Generated from **Poly[(*3,4-3,5*)*m*G2−4EBn]** Cylindrical Macromolecules

polymer	*T* (°C)	lattice	*d* spacings (Å)				a^a (Å)	$\rho_{20}{}^b$ (g/cm^3)	μ^c
			d_{100}	d_{110}	d_{200}	d_{210}			
poly[(*3,4*-3,5)8G2−4EBn]	−20	*p6mm*	38.2	22.1	19.3		44.3	1.019	4.94
	60	*p6mm*	38.6	22.3	19.4		44.7		
	105	*p6mm*	35.4	20.4	17.7		40.8		
poly[(*3,4*-3,5)dm8G2−4EBn]	23	*p6mm*	37.0	21.4	18.8		43.0	–	–
	50	*p6mm*	36.3	21.0	18.4		42.1		
	100	*p6mm*	35.0	20.2	17.6		40.5		
poly[(*3,4*-3,5)10G2−4EBn]	25	*p6mm*	40.6	23.4	20.4		47.0	1.009	5.0
	70	*p6mm*	40.5	23.4	20.3		46.9		
	105	*p6mm*	38.3	22.1	19.2		44.0		
poly[(*3,4*-3,5)12G2−4EBn]	30	*p6mm*	43.7	25.2	22.0		50.6	1.014	5.25
	70	p6*mm*	43.2	24.9	21.7		49.6		
	105	*p6mm*	38.9	22.4	19.5		44.9		
poly[(*3,4*-3,5)14G2−4EBn]	30	*p6mm*	46.0	26.5	23.3		53.2		
	70	*p6mm*	45.1	25.8	22.7		52.0		
	100	*p6mm*	40.7	23.2	20.5		46.9		
poly[(*3,4*-3,5)16G2−4EBn]	30	*p6mm*	47.2	27.6	24.0	18.0	55.1	1.005	5.25
	70	*p6mm*	47.3	27.2	23.7		54.6		
	105	*p6mm*	42.2	24.4	21.1		48.7		

[a] Lattice parameter, $a = 2\langle d_{100}\rangle\sqrt{3}$, where $\langle d_{100}\rangle = (d_{100} + \sqrt{3}d_{110} + 2d_{200} + \sqrt{7}d_{210})/4$; for columnar phases, the lattice parameter (a) and diameter of the column (D_{col}) are equal. [b] ρ_{20}, experimental density measured at 20 °C. [c] Number of dendrons in a column stratum = $(\sqrt{3}N_A a^2 t\rho_{20})/2M$, where Avogadro's number $N_A = 6.0220455 \times 10^{23}$, layer thickness $t = 4.7$ Å, and M is the molecular weight of the monomer.

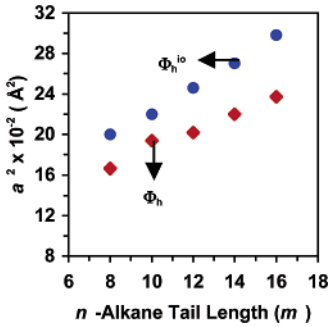

Figure 1. Square of the lattice parameter (a^2) as a function of the number of methylenic units (m). The steepest increase is observed for the low-temperature range (determined between 60 and 70 °C) when the aliphatic tails are more rigid. In the high-temperature phase (determined from 100 and 105 °C, Table 3) the alkyl tails are more flexible, allowing a repacking of the dendrons.

columnar order that involves helicity, well-defined dendron tilt, and other features that give rise to diffuse XRD peaks. Due to the liquidlike aliphatic coat, the intracolumnar order is not correlated from one column to another in the $\Phi_h{}^{io}$ phase. Figure 1 compares the square of the experimental lattice parameter (a^2), which is analogous to the square of the column diameter ($D_{col}{}^2$), with the number of methylenic units (m) in the *n*-alkane chains. In agreement with the microphase-segregated model, the linear fit of the experimental data indicates that the density of the aliphatic region of the column is constant for all measured chain lengths. Since, as will be discussed later, the lattice dimensions are temperature dependent, the trend from Figure 1 is only qualitative. Nevertheless, it demonstrates a marked difference between column diameters in the $\Phi_h{}^{io}$ and Φ_h phases.

XRD Patterns of oriented fibers of all dendronized PPAs exhibit a feature at 6.5 ± 0.2 Å that indicates intracolumnar helical order in the $\Phi_h{}^{io}$ phase. This feature persists through any phase transition observed by DSC, except the highest temperature transition (Figure 2). Furthermore, this feature is recovered on cooling. In the case of **(*3,4-3,5*)16G2−4EBn**, the diffraction pattern of the oriented fiber in the $\Phi_h{}^{io}$ phase shows, besides the first-order feature at 6.6 Å, a diffuse weak second-order helical feature at 13.5 ± 0.2 Å (Figure 2). This demonstrates that the first-order feature observed in the other samples at 6.5 ± 0.2 Å is due to intracolumnar helical order. CD spectra of **poly[(*3,4-3,5*)dm8G2−4EBn]** in methyl cyclohexane at 2 °C and 22 °C further support the presence of a helical conformation in the polymer backbone in solution (Figure 3). The decrease of the Cotton effect intensity at elevated temperatures is consistent with the dynamic helical behavior observed in cis−transoidal PPAs.[13] Since at the transition from solution to solid-state XRD data show that the dendronized polymer maintains its helical conformation, the helix sense selected by the stereocenter in solution is preserved in solid state.

XRD patterns obtained during heating and cooling cycles indicate that the lattice parameter undergoes a discontinuous and sudden change that is both reversible and reproducible. Figure 4a,b presents plots of D_{col} over a range of temperatures with the corresponding DSC traces showing the high-temperature transition on heating and cooling cycles. Furthermore, the angle at which the dendron tilts relative to the column axis is ∼40° for all alkyl chain lengths in the low-temperature $\Phi_h{}^{io}$ phase. The change in D_{col} at the DSC phase transition (Figure 4a,b) is responsible for the difference observed in the trend from Figure 1.

The reconstructed electron density maps for **poly[(*3,4-3,5*)-12G2−4EBn]** in the $\Phi_{h,k}$ phase at 20 °C, in the $\Phi_h{}^{io}$ at 50 °C, and in the Φ_h phase at 110 °C were calculated from the XRD data with the following phase choice for the four diffraction peaks of the hexagonal columnar phase: (10) +, (11) −, (20) −, and (21) −. The electron density maps of the $\Phi_{h,k}$ and $\Phi_h{}^{io}$ phases are almost identical. Figure 5 shows the electron density maps in the $\Phi_{h,k}$ phase at 20 °C and in the Φ_h phase at 110 °C. The electron density maps from Figure 5 support the intracolumn phase-segregated model. The electron density map of the lower-temperature $\Phi_{h,k}$ and $\Phi_h{}^{io}$ phases exhibits a drop in electron density at the column core. The significance of such an observation has recently been discussed for a series of self-assembling dendritic dipeptides.[8] In the $\Phi_{h,k}$ and $\Phi_h{}^{io}$ phases,

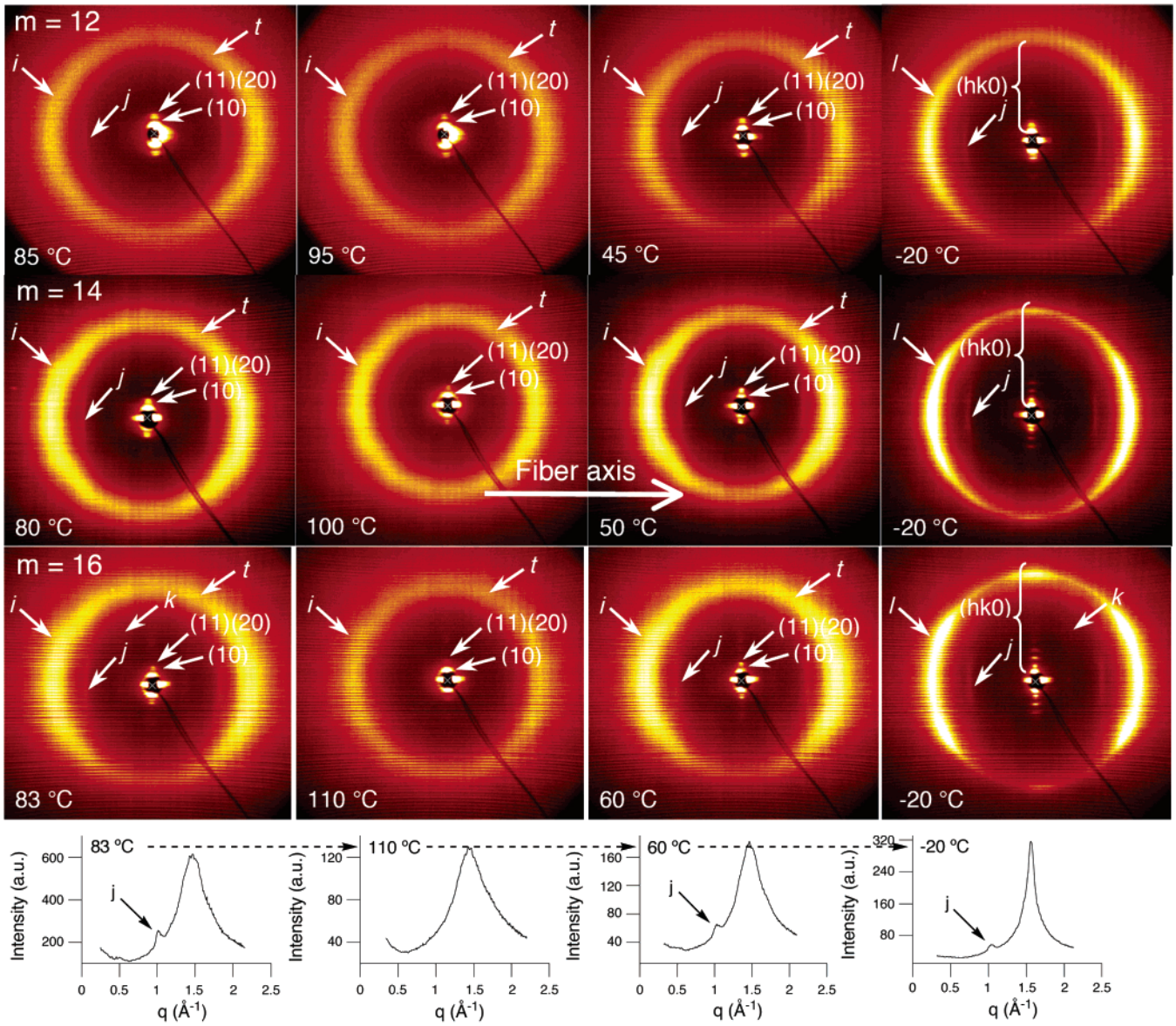

Figure 2. Wide-angle diffraction patterns of aligned fibers (horizontal fiber axis is indicated by arrow) collected in the temperature sequence indicated by the dotted arrows for **poly[(*3,4-3,5*)*m*G2−4EBn]** with $m = 12, 14, 16$. $q = (4\pi/\lambda)\sin\theta$ is the momentum transfer. *i*, four diffuse X-shape short-range helical features (4.4 ± 0.2 Å); *j*, 6.5 ± 0.2 Å first-order helical features (corresponding to the dendron registry along the column axis); *k*, four X-shape diffuse spots corresponding to the 13.5 ± 0.2 Å second-order helical feature (slightly enhanced for **poly[(*3,4-3,5*)16G2−4EBn]** at −20 °C) (see Figure 6); *l*, average stratum thickness in the $\Phi_{h,k}$ phase (4.1 ± 0.2 Å); *t*, four diffuse X-shape features due to dendron tilt (57 ± 9°); (*hk*0), higher-order reflection of the hexagonal columnar phase. Diffractionlike spots near the beam stop on the equators are from the beam stop.

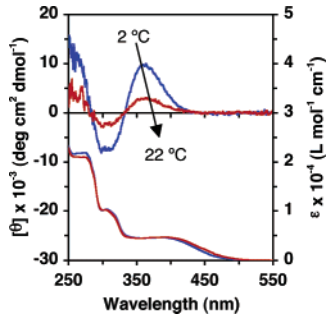

Figure 3. Circular dichroism (top, left axis) and UV−vis spectra (bottom, right axis) of **poly[(*3,4-3,5*)dm8G2−4EBn]** in methyl cyclohexane ([**4EBn**] = 9.1 × 10^{-4} M) at 2 (blue curves) and 22 °C (red curves).

the columns have a small pore of 3.8 ± 1.2 Å. The size of the pore was calculated from the intensity of the X-ray diffraction peak data collected at 20 °C by using the procedure reported previously.[8] In the highest-temperature Φ_h phase, this feature is absent from the electron density map, indicating that the helical conformation is compressed (cis−cisoisal) in the low-temperature $\Phi_{h,k}$ and Φ_h^{io} phases and stretched (cis−transoidal) in the high-temperature Φ_h phase. This difference is in agreement with the difference between the cis−cisoidal and cis−transoidal conformations of pristine PPA, as well as with the difference between D_{col} in the two phases (Figure 1).

Structural Model. In combination with the observations above, molecular modeling studies constrained by the XRD results clarify the significance of the Φ_h^{io}-to-Φ_h phase transition. Given a helical conformation of the polymer backbone, the dihedral angle (β) associated with the cisoidal and transoidal conformations in cis−PPA is the only available mechanism to explain the observed column pore and its disappearance at elevated temperature. Two such angles are illustrated in Figure

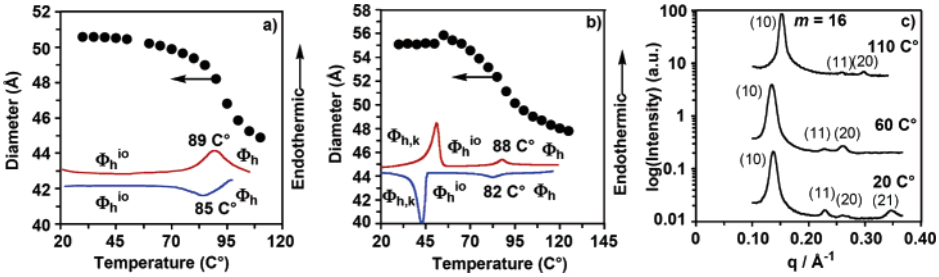

Figure 4. (a) Temperature dependence of the column diameter and the corresponding DSC traces (red, heating; blue, cooling) for **poly[(*3,4-3,5*)*m*G2−4EBn]** ($m = 12$); (b) same data for $m = 16$. (c) Representative small-angle XRD plots for **poly[(*3,4-3,5*)16G2−4EBn]**, indicating an enhancement of the (11) and (21) peaks in the $\Phi_{h,k}$ and Φ_h^{io} phases at 20 and 60 °C compared to the Φ_h phase at 110 °C.

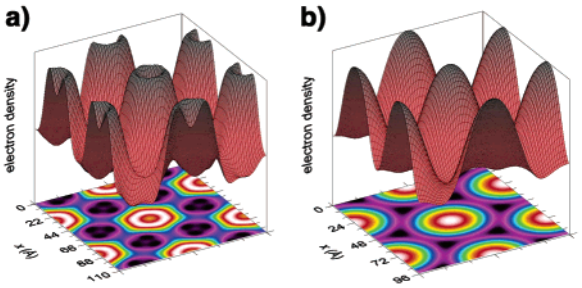

Figure 5. Electron density maps reconstructed from the XRD data of **poly-[(*3,4-3,5*)12G2−4EBn]** (a) in the $\Phi_{h,k}$ phase at 20 °C and in the Φ_h^{io} at 50 °C and (b) in the Φ_h phase at 110 °C.

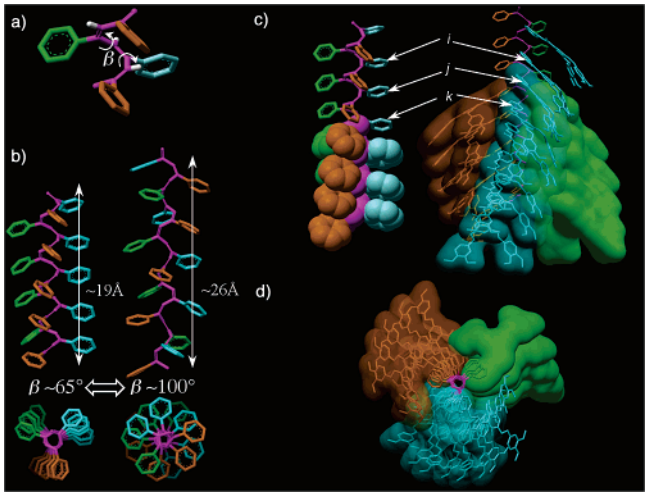

Figure 6. Models illustrating (a) the dihedral angle (β) about the single bond in the polyene backbone, (b) side and top views of PPA oligomers with $\beta \approx 65°$ (cis−cisoidal) and 100° (cis−transoidal) and the corresponding change in length along the helix axis, (c) side views of space-filling models of PPA and **poly[(*3,4-3,5*)*m*G2−4EBn]** showing the helical registry of aromatic rings that explains the 6.6 ($i-j$) and 13.5 Å ($i-k$) helical features in the Φ_h^{io} phase (see Figure 2), and (d) a top view of a space filling model of **poly[(*3,4-3,5*)*m*G2−4EBn]** with low-electron-density core.

6 from both top and side views. The side views indicate a corresponding stretch of the helix axis. Furthermore, when $\beta \approx 65°$ (i.e., cis−cisoidal PPA), the aromatic rings of the PPA backbone are in registry consistent with the observed 6.6 Å features in the fiber XRD patterns. When $\beta \approx 100°$ (i.e., cis−transoidal PPA), the registry is not apparent. Appending the dendrons to the polymer backbone in a conformation that both creates a 40° tilt relative to the column axis and adequately fills space creates an aromatic core whose diameter matches that calculated above. Increasing β results in a larger tilt angle and, together with contraction of the alkyl tails, a smaller column diameter.

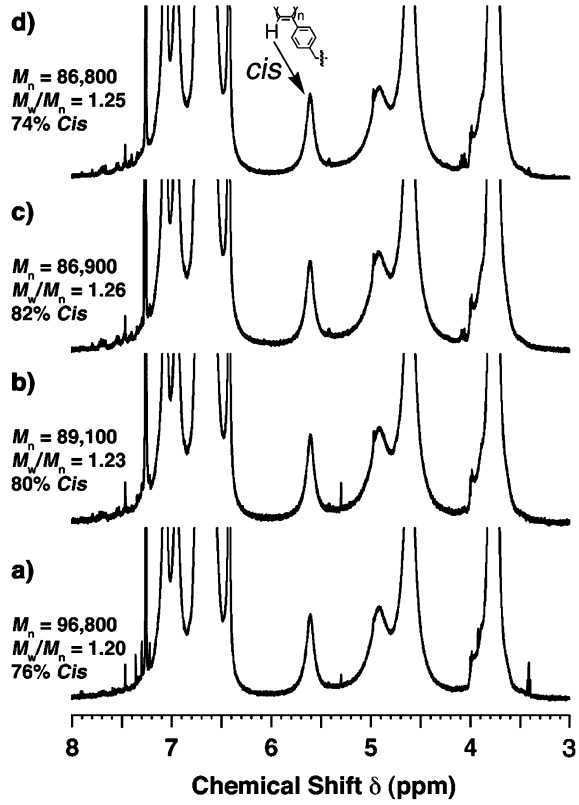

Figure 7. ^{1}H NMR Spectra and GPC data for (a) pristine **poly[(*3,4-3,5*)-12G2−4EBn]** and samples annealed (b) under argon at 100 °C for 30 min, (c) in air at 100 °C for 30 min, and (d) in air at 85 °C for 3 h. Cis content determined as described in ref 12a.

Thermal Stability. In bulk or solution, thermally induced 6π electrocyclization of 1,3-*cis*,5-hexatriene sequences in cis-PPA to form cyclohexadiene repeat units occur via the cisoidal conformation.[12] While very little cyclization is observed at room temperature in bulk, the rate of cyclization increases with temperature and becomes significant above 60 °C. Furthermore, at temperatures above 120 °C, extrusion of triphenylbenzene with concomitant chain cleavage is observed due to re-aromatization of cyclohexadiene repeat units.[12] The temperature-triggered relaxation (unwinding) of the PPA backbone upon heating is expected to eliminate the intramolecular cyclization reaction.

The stability of these polymers toward thermal cycling was investigated. A fiber sample of **poly[(*3,4-3,5*)10G2−4EBn]** extruded at 95 °C and cycled during XRD experiments between 50 and 100 °C over 3.5 h was dissolved in THF, and its molecular weight (M_n) and molecular weight distribution (M_w/

M_n) were determined by GPC. The initial values are reported in Table 1, and for the thermally treated sample, $M_n = 101\,000$ and $M_w/M_n = 1.30$. Films of **poly[(*3,4-3,5*)12G2−4EBn]** cast from CH_2Cl_2 were thermally treated under several conditions. Figure 7 illustrates ^1H NMR spectra of the pristine polymer, as well as a film annealed at 100 °C under anaerobic conditions for 30 min and films annealed under ambient atmosphere at 100 °C for 30 min and at 85 °C for 3 h. The measured cis content and GPC results show nominal differences. The steric demand of the dendron provides a driving force against intramolecular 6π electrocyclization in bulk samples.

Conclusions

From a library of dendronized cis−transoidal PPAs, we have selected a dendritic architecture whose match to the helical pitch of the polymer backbone allowed a detailed structural and retrostructural analysis of the dendronized PPA. Variation of the peripheral alkyl tails has led to a quantitative analysis of the structure, the results of which are in agreement with a microphase-segregated model for the cylindrical PPA. XRD experiments have clarified the internal structure. In the $\Phi_{h,k}$ and Φ_h^{io} phases, the dendrons are titled at ~40° to a helical porous column axis. Solution CD experiments demonstrate the selection of a single-handed helix sense by incorporation of dendritic homochiral tails. In bulk, a Φ_h^{io}-t-Φ_h phase transition was identified as a temperature-triggered relaxation of the polymer backbone, which leads to a transition from a compressed helical porous structure to a stretched helical nonporous structure. A combination of XRD, electron density calculations, and molecular modeling studies was used to explain this process by an unprecedented cis−cisoidal-to-cis−transoidal conformational isomerization of the dendronized cis-PPA. The thermoreversible stretching of the polymer backbone impedes the intramolecular 6π electrocyclization encountered in annealed pristine cis-PPA samples and provides a gating mechanism for the helical porous structure.

Acknowledgment. Financial support by the National Science Foundation (DMR-99-96288 and DMR-01-02459) is gratefully acknowledged.

Supporting Information Available: Experimental part containing materials, methods, synthesis, and structural analysis and additional XRD patterns from oriented fiber samples. This material is available free of charge via the Internet at http://pubs.acs.org.

JA055406W